JAREE (2026), Vol. 10, No. 1
doi: 10.12962/jaree.xyzxyz

JAREE Journal on Advanced Research in Electrical Engineering
ISSN: 2579-6216

RESEARCH ARTICLE

An Active Balancing for Liquid Metal Battery Using Bidirectional Flyback Converter with Fuzzy Logic Control

M. Zainul Muttaqi[1] , Feby Agung Pamuji*

[1] Department of Electrical Engineering, Institut Teknologi Sepuluh Nopember, Surabaya, Indonesia

*Corresponding author (feby@ee.its.ac.id).

Received: 31 May 2025; **Revised:** 24 July 2025; **Accepted:** 24 July 2025

Abstract

Batteries are increasingly in demand with the growing use of renewable energy. Lithium-ion (Li-ion) batteries are currently the most widely used type of battery due to their high energy density; however, their short lifespan (1,500–4,500 cycles) results in significant environmental waste. Liquid metal batteries (LMB) offer a promising alternative, with a lifespan of up to 10,000 cycles, high energy density, and simpler thermal management. Since LMBs operate at low voltages, these batteries must be connected in series configurations to meet system requirements. However, batteries connected in series often experience capacity imbalances, preventing them from being utilized at their maximum capacity because the system is limited by the cell with the highest state of charge (SoC) during charging and the cell with the lowest SoC during discharging. Active balancing is crucial to minimize energy loss, especially in high-capacity batteries like LMB. Bidirectional active balancing, which uses a flyback converter, is the optimal solution due to its high speed and efficiency. Additionally, a fuzzy logic controller (FLC) is applied due to its simplicity and ability to operate without complex mathematical models. The experimental results show that this method achieves rapid balancing in three test cases (1.05 seconds, 1.341 seconds, and 1.968 seconds), outperforming conventional unidirectional balancing by 35–40% in convergence speed. The proposed bidirectional active balancing system has proven to be an effective solution for improving the performance and service life of LMB-based energy storage systems.

Keywords: bidirectional flyback converter, fuzzy logic, liquid metal battery

I. INTRODUCTION

With the increasing use of renewable energy, the demand for batteries has skyrocketed over time. Li-ion batteries are the most widely used because they have a higher energy density compared to others. However, this battery has problems related to its life cycle, which only reaches 1500-4500 or 2-3 years of normal use [1]. This battery also can explode when thermal runaway problems occur [2]. Liquid Metal Batteries (LMBs) have emerged as a promising alternative to address this limitation. LMB features a three-layer structure comprising liquid metal electrodes and liquid salt electrolytes, providing a reliable energy storage solution. This fully liquid configuration eliminates solid electrode degradation, offers cost efficiency, and provides intrinsic safety. By avoiding mechanical failure modes associated with solid electrodes, LMB achieves a long operational lifespan of up to 20 years, simple assembly, and passive thermal resistance, making it a promising alternative for grid-scale storage [3,4].

LMBs operate within a voltage range of 0.5 V to 1.4 V, with capacities ranging from 50 Ah to 500 Ah. Due to these characteristics, LMB cells cannot operate independently and must be arranged in series and parallel configurations to meet specific energy and power demands [5]. Nonetheless, the series connection of LMB cells may result in discrepancies in the State of Charge (SoC), which is detrimental to the overall performance and longevity of the battery. Cells with an elevated SoC risk being overcharged during charge cycles, which may result in overheating as well as severe damage. Similarly, during discharging, cells with a lower SoC may experience over-discharge, which could degrade the cells and shorten their lifespan. A balancing process is required to maintain balanced SoC levels across all cells [6]. There are two methods for balancing: passive and active [7].

Passive balancing is a resistor-based equalization technique that does not utilize power converters. Instead, it employs shunt resistors controlled by switches to dissipate excess energy from cells with a higher state of charge (SoC). When activated, the switch allows current to flow through the resistor, reducing the overcharged cell's energy until its SoC aligns with the other cells in the pack. Although this method offers simplicity and low cost, its energy inefficiency—due to heat dissipation—makes it unsuitable for large-capacity battery systems, such as LMB [8].

Active balancing utilizes power electronic components, such as inductors, capacitors, or DC-DC converters, to redistribute energy from cells with higher state-of-charge (SoC) to those with lower SoC within a battery pack. This method enables efficient energy transfer between cells while minimizing energy losses compared to passive balancing techniques [9]. Active balancing uses capacitors or inductors to transfer energy between cells through a series of switches. However, this method has a significant drawback: balancing time increases when cells with an overcharged state of charge (SoC) are located far from cells with a low SoC. In contrast, balancing cells with a low SoC offers the advantage of being

How to cite: Muttaqi, M.Z., & Pamuji, Feby Agung., (2026). An Active Balancing for Liquid Metal Battery Using Bidirectional Flyback Converter with Fuzzy Logic Control. JAREE (Journal on Advanced Research in Electrical Engineering), Volume 10 (No.1).

time-independent, as it does not depend on the distance between overcharged and undercharged cells [10].

There are various types of balancing methods that utilize converters. One that can be used is a converter that can be achieved by transferring energy from the entire battery pack to individual cells with a lower SoC using a flyback converter. However, this method presents a drawback: it is less efficient when the number of cells with excess SoC significantly exceeds those requiring charge. Alternatively, energy can be transferred in the opposite direction from overcharged cells to the pack to achieve balance. However, this approach introduces a complementary limitation: if cells with low SoC outnumber those with high SoC, the balancing process becomes prolonged. A bidirectional flyback converter resolves these inefficiencies by enabling energy transfer in both directions. This flexibility eliminates the key disadvantages of unidirectional balancing methods, ensuring faster and more adaptable cell equalization regardless of charge distribution [11]. In addition to having a fast balancing time, the two-way converter also has high efficiency, reaching up to 96.8% [12].

To regulate the switching of converter-based active balancing systems, an effective control strategy is required. One suitable approach is Fuzzy Logic Control (FLC), which offers notable advantages, including the elimination of complex mathematical modeling and robust performance in nonlinear systems. FLC has been successfully implemented as an active balancing controller for lithium-ion batteries using a buck-boost converter topology. In a case study involving nine series-connected cells with a maximum state-of-charge (SoC) deviation of 28%, the FLC-controlled converter achieved voltage balance within 2,672 seconds, demonstrating its effectiveness in managing significant charge disparities [13].

Based on the preceding discussion, this study proposes an active balancing solution for lithium metal batteries (LMBs) utilizing a bidirectional flyback converter, a topology that has been demonstrated to achieve rapid balancing in Li-ion batteries, combined with Fuzzy Logic Control (FLC). This approach has been empirically validated for Li-ion systems with buck-boost converters. To verify the efficacy of this approach, the proposed system will be simulated using PSIM software, enabling performance evaluation under controlled conditions.

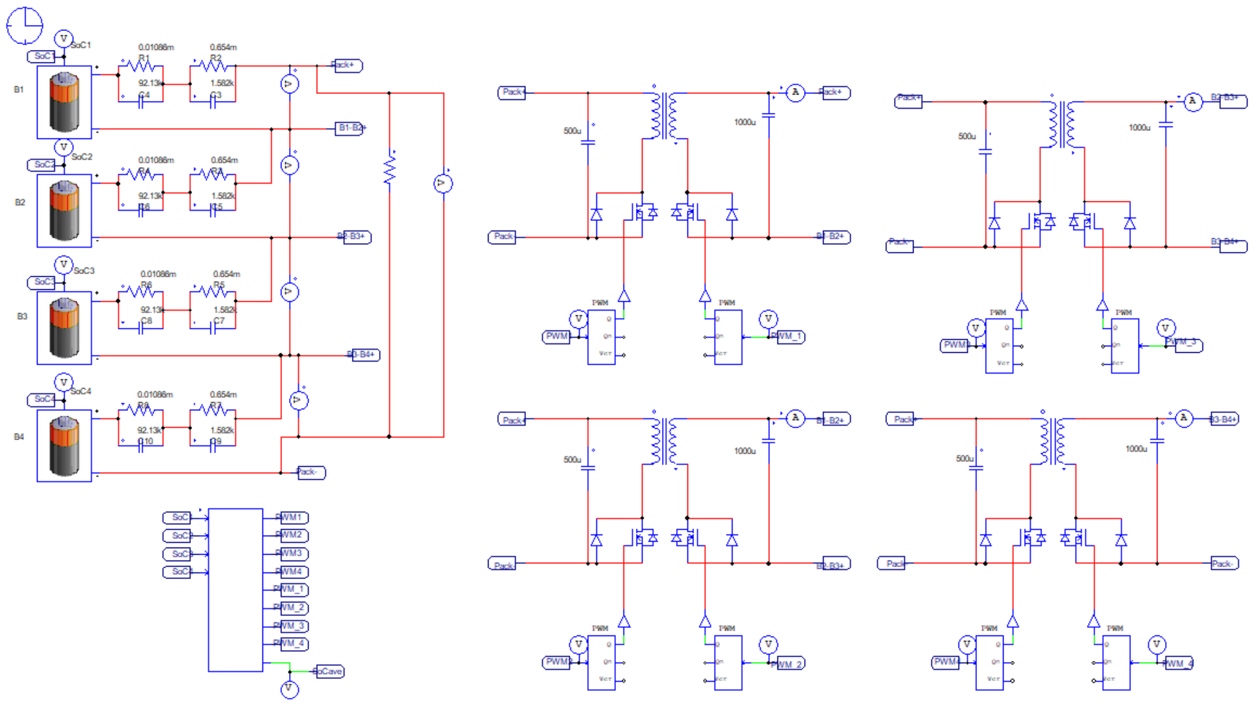

Fig. 1 LMB balancing using BFC with FLC

II. Methods

Battery modeling and LMB balancing system design were simulated using PSIM software. Fig. 1 shows the balancing system circuit using BFC. The left image shows four battery cells arranged in series, with the C block below containing the FLC program. The right image shows four BFCs, with the left side connected to the pack and the right side connected to each cell terminal.

A. Modeling Liquid Metal Battery

Liquid Metal Batteries (LMB) have distinct characteristics compared to other types of batteries, as they utilize electrodes made of metal materials that are heated to a liquid state. As shown in Fig. 2, an LMB in its fully charged state consists of three liquid layers. The topmost and bottom layers serve as the cathode and anode, respectively, in liquid form. In this system, liquid Lithium (Li) functions as the cathode, while liquid Bismuth (Bi) serves as the anode. Lithium chloride, in its molten state, acts as the electrolyte and as a separator between the two electrodes. These three layers have different densities, preventing them from mixing [14].

During discharge, lithium (Li) metal at the anode oxidizes, releasing Li^+ ions into the molten LiCl electrolyte and electrons to the external circuit. Simultaneously, at the cathode, bismuth (Bi) reacts with the incoming Li^+ ions and electrons to form a lithium-bismuth intermetallic alloy (LiBi or Li_3Bi). The overall discharge reaction is:

$$Li + Bi \rightarrow LiBi + Energy$$

During charging, an external voltage is applied to reverse the discharge reactions. At the cathode, the lithium-bismuth intermetallic alloy (LiBi or Li_3Bi) decomposes, releasing Li^+ ions into the molten LiCl electrolyte and electrons into the external circuit. Concurrently, at the anode, Li^+ ions from the electrolyte accept electrons and are reduced back to metallic lithium (Li). The overall charge reaction is:

$$LiBi + Energy \rightarrow Li + Bi \text{ [15]}$$

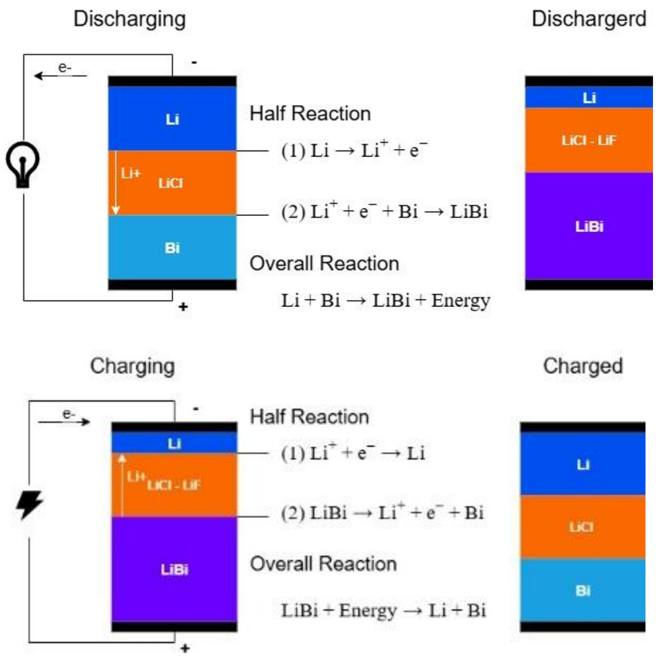

Fig.2. Schematics of LMB

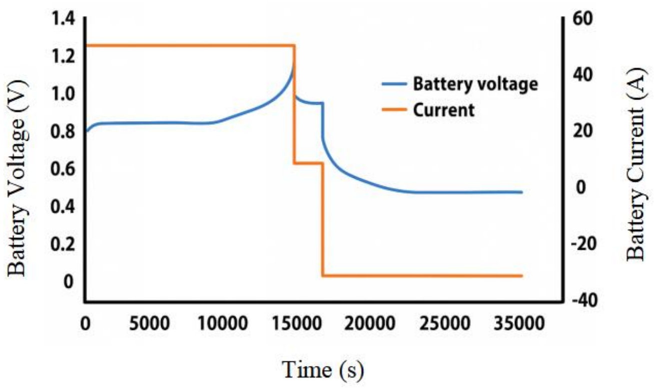

Fig. 3 Voltage-current charge and discharge curve of LMB [16]

LMBs offer several advantages over other battery technologies, one of which is their large capacity. Fig. 3 illustrates the charge and discharge curve of a single LMB cell. The Figure demonstrates that a single LMB cell, with a charging or discharging current of 50 A, takes 15,000 seconds (or more than 4 hours) for a full cycle. Based on these parameters, the capacity of one LMB cell is calculated to be 208.33 Ah. The curve also shows that the working voltage of the LMB cell ranges from 0.8 V to 1.2 V [16].

Modeling of the Liquid Metal Battery (LMB) in this study represents the battery as a second-order Thevenin circuit, as shown in Fig. 4. This model illustrates the equivalent circuit of the battery, which includes the open-circuit voltage (U_{OCV}), the internal resistance of the battery (R_o), and the parallel components R_1 and R_2, as well as R_2 and C_2.

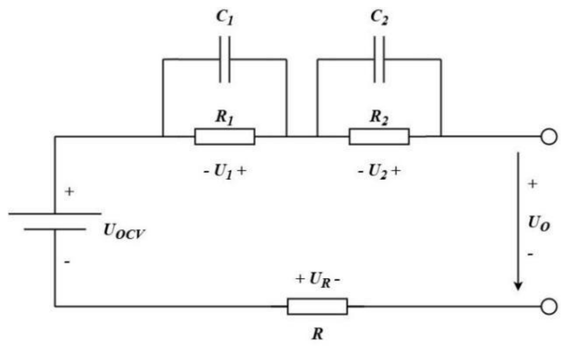

Fig. 4. Equivalent circuit of LMB

Both UOCV and Ro vary with the state of charge (SoC) of the battery. The values of these parameters change over time, as demonstrated by the curves of U_{OCV} and Ro as functions of SOC, shown in Fig. 5 and Fig. 6. The values of R_1, C_1, R_2, and C_2, however, are kept constant, as indicated in Table 1 [14].

TABLE I. THE VALUE OF SECOND ORDER THEVENIN R AND C

	R_1(mΩ)	R_2(mΩ)	C_1(kF)	C_2(kF)
Value	0.01086	0.654	92.13	1.582

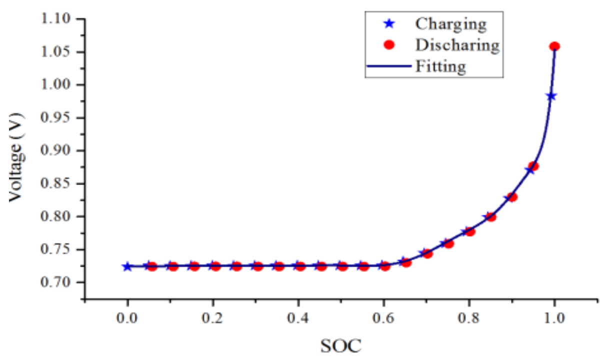

Fig. 5. OCV – SOC curve of LMB [11]

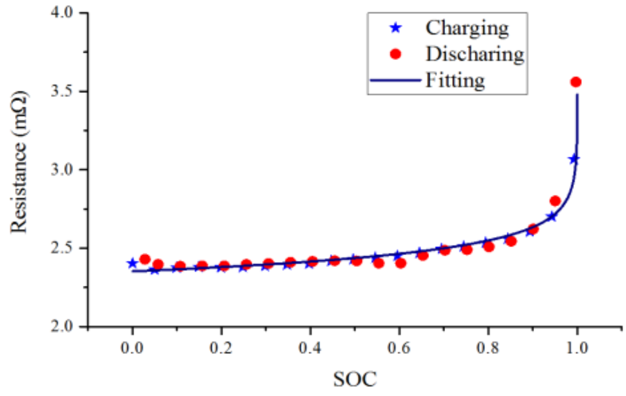

Fig. 6. Internal resistance (Ro) – SOC curve of LMB [14]

The LMB battery model is simulated using a battery library with a lookup table approach implemented in PSIM software. The equivalent circuit for this type of battery consists of a voltage source and internal resistance, with values derived from the OCV-SoC table and R-SOC curves shown in Fig. 4 and Fig.5. The values for R_1, R_2, C_1, and C_2 are added manually to complete the battery model, as shown in the simulation circuit diagram in Fig 7.

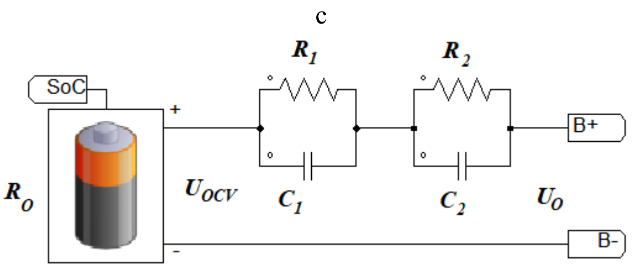

Fig. 7. LMB schematic on PSIM

B. Design of Bidirectional Flyback Converter

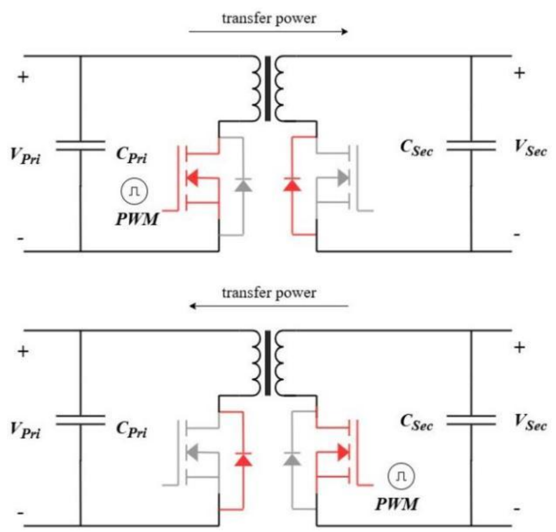

Fig. 8. Bidirectional flyback converter schematic [17]

The Bidirectional Flyback Converter (BFC) is a modification of the traditional flyback converter circuit, which incorporates a MOSFET as a switch on the secondary side of the transformer and utilizes the internal diodes of the MOSFETs instead of the unidirectional diodes typically used in conventional flyback converters. Fig. 8 illustrates the operation of this converter. When the desired power flow is from the primary side to the secondary side, the primary MOSFET (Q_{pri}) is turned on while the secondary MOSFET (Q_{sec}) is turned off or behaves as a diode. Under these conditions, the secondary voltage to be regulated has a value as shown in equation (1).

$$V_{sec} = V_{pri}\left(\frac{D}{(1-D)}\right)\left(\frac{N_{sec}}{N_{pri}}\right) \quad (1)$$

Where D is the duty cycle of PWM, V_{pri} is the voltage on the primary side of the converter, N_{sec} is the number of turns on the secondary side of the transformer, and N_{pri} is the number of turns on the primary side of the transformer.

When the desired power flow is from the secondary side to the primary side, Q_{sec} is activated, and Q_{pri} functions as a diode [17]. Under these conditions, the secondary voltage to be regulated has a value as shown in equation (2). The voltage levels set on both the primary and secondary sides are influenced by the transformer ratio and duty cycle in PWM.

$$V_{pri} = V_{sec}\left(\frac{D}{(1-D)}\right)\left(\frac{N_{pri}}{N_{sec}}\right) \quad (2)$$

C. Modeling Fuzzy Logic Controller

The Fuzzy Logic Controller (FLC) uses fuzzy set theory in its design. Both the input and output of the control system are fuzzy sets with specific membership functions. The block diagram of the FLC system is depicted in Fig. 8.

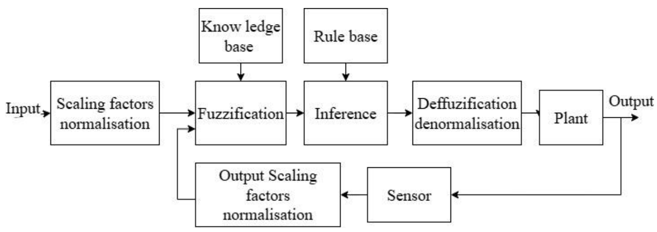

Fig 9. Block diagram of the Fuzzy Logic Controller [18].

There are five basic elements in an FLC:

1. Fuzzification

Fuzzification converts the crisp values of the control inputs into fuzzy values, assigning membership degrees based on the MF. These fuzzy values correspond to the fuzzy set representations in the rule base. There are two inputs in the applied FLC design: deviation and delta deviation. Deviation here is the value of the difference between the SoC of one cell and the average SoC of all cells. At the same time, delta deviation is the difference between the deviation before and after the FLC system works. Fig. 10 displays the membership operations applied in this system. Both inputs use two trapezoids and three triangles as MFs.

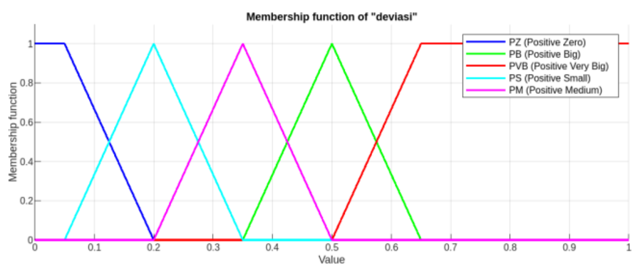

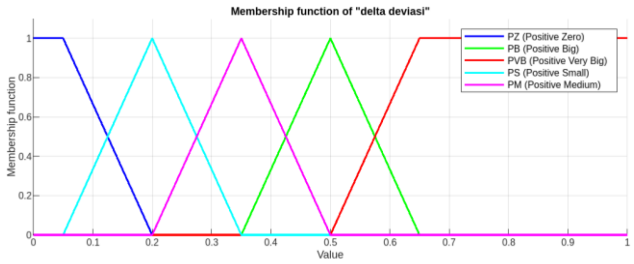

(a) MF for the primary side of the Flyback converter

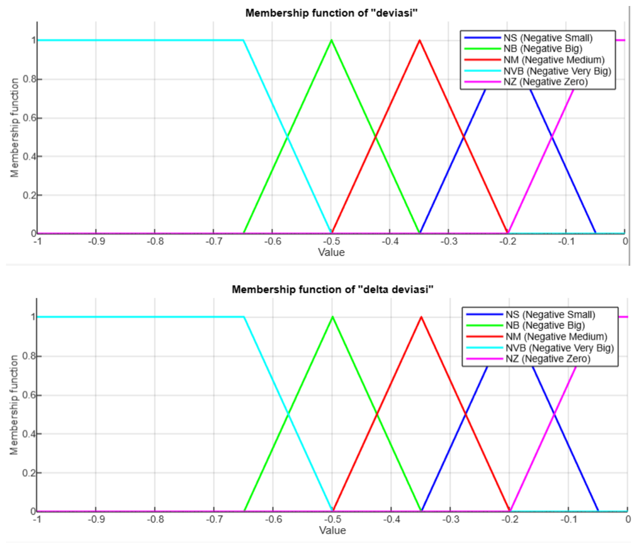

(b) MF for the secondary side of the Flyback converter

Fig. 10. Inputs membership function

2. Knowledge Base

The knowledge base consists of a database that provides all the definitions necessary for the fuzzification process, such as the membership functions, fuzzy set representations of input-output variables, and mapping functions between the physical domain and the fuzzy domain.

3. Rule Base

The rule base contains the control strategies for the system, typically derived from expert knowledge or heuristics. These are expressed as a set of "if-then" rules based on fuzzy inference concepts associated with linguistic variables. For example: If the deviation and delta deviation are very big negative, then the PWM og BFC is very high. Table II shows the basis of the rules used in this study.

TABLE II. THE RULE BASE OF FLYBACK CONVERTER PRIMARY SIDE FLC

Del_dev \ Dev	NVB	NB	NM	NS	NZ
NVB	VH	VH	VH	H	M
NB	VH	H	H	M	M
NM	VH	H	M	M	L
NS	VH	M	M	L	VL
NZ	H	L	L	L	VL

Description

NVB : Very Big Negative

NB : Big Negative

NM : Middle Negative

NS : Small Negative

NZ : Zero Negative

TABLE III. THE RULE BASE OF FLYBACK CONVERTER SECONDARY SIDE FLC

Del_dev \ Dev	PVB	PB	PM	PS	PZ
PVB	VH	VH	VH	H	M
PB	VH	H	H	M	M
PM	VH	H	M	M	L
PS	VH	M	M	L	VL
PZ	H	L	L	L	VL

Description

PVB : Very Big Positive

PB : Big Positive

PM : Middle Positive

PS : Small Positive

PZ : Zero Positive

4. Inference Engine

The inference engine processes the fuzzy inputs according to the rules in the rule base and derives the fuzzy output.

5. Defuzzification

Defuzzification is the process of converting fuzzy numbers back into crisp values. Several methods are used in defuzzification, one of which is the Sugeno method. This method is easier to implement in programming languages because it uses a singleton set for the output variable. The output equation of the Sugeno method is as follows equation (15). The membership function used in this system is shown in Fig. 11.

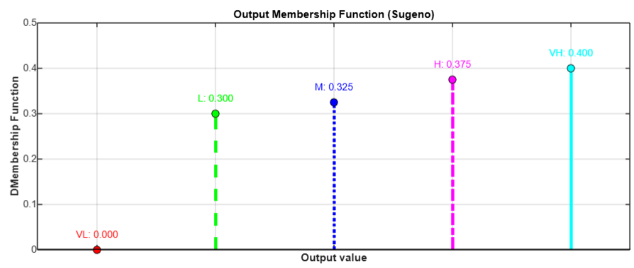

(a) The output MF on the primary side FLC

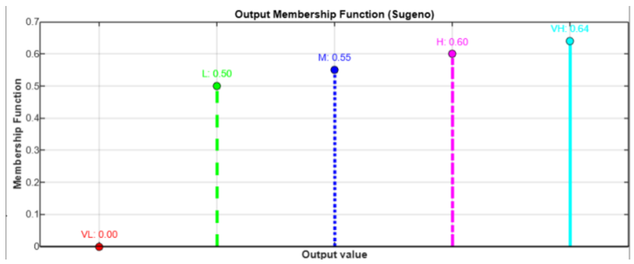

(b) The output MF on the secondary side FLC

Fig. 11. Outputs membership function

$$z_{out} = \frac{\sum_{i=1}^{n} w_i z_i}{\sum_{i=1}^{n} w_i} \quad (15)$$

Where n is the number of fuzzy rules. w_i is the firing strength (activation level) of rule i, calculated from the AND (min) or OR (max) operation of the input membership degrees. z_i is the output of rule i (can be a constant or a linear function).

III. Results and Discussions

To test the effectiveness of LMB balancing using BFC with FLC, the system was simulated in three cases, each with different SoC characteristics for each cell.

A. First Case

The State of Charge (SoC) distribution across individual cells and their respective deviations from the average value are presented in Table 4. In the first case, only Cell 2 exhibits a significantly higher SoC value compared to the other cells in the system, resulting in this cell being the sole unit with a positive deviation. The corresponding simulation results are illustrated in Fig. 12.

TABLE IV. THE SOC OF EACH SEL IN THE FIRST CASE

Cell	SoC	deviation
1	75.70 %	-0.55
2	75.99 %	0,235
3	75.68 %	-0,075
4	75.65 %	-0,105

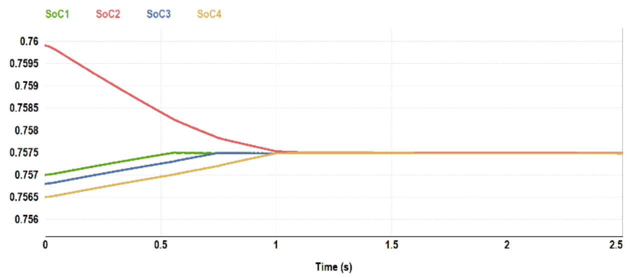

a) Battery SoC with Bidirectional Converter

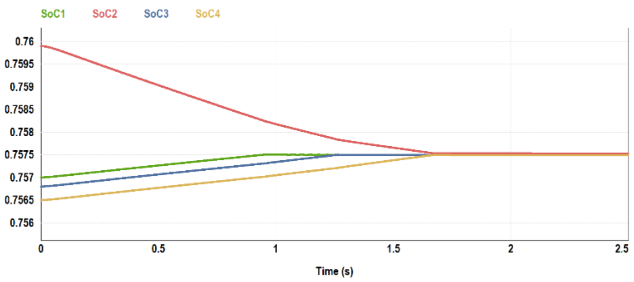

(b) Battery SoC with Pack to Cell Converter

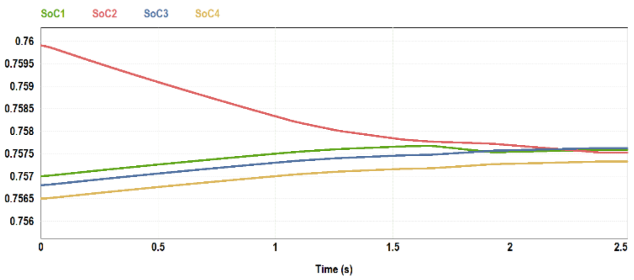

(c) Battery SoC with Cell to Pack Converter

Fig. 12. SoC of the battery in the first case

The time required to achieve balance for each controller is shown in Table 5, and the current for each cell is shown in Table 6.

TABLE V. THE TIME TO REACH BALANCE STATE IN THE FIRST CASE

Converter	Time (s)
Bidirectional	1.05
Pack to Cell	1.68
Cell to Pack	Not reach

TABLE VI. CURRENT OF EACH CELL IN THE FIRST CASE

Cell	Average Current (A)		
	Bidirectional	**Pack to Cell**	**Cell to Pack**
1	9.973	6.626	-0.472
2	-0.252	0.507	-4.926
3	10.689	7.043	-0.117
4	11.762	7.6854	-0.117

The SoC evolution curves reveal significant differences in balancing performance among converter topologies. As shown in Table 5 the bidirectional converter achieves balanced conditions most rapidly, reaching equilibrium in 1.05 seconds—37.5% faster than the pack-to-cell converter (1.68 seconds)—while the cell-to-pack configuration fails to attain balance within the 2.5-second observation window. Current response shown in Table 6 analysis demonstrates that the bidirectional converter facilitates simultaneous charge redistribution through dual-directional energy transfer, supplying positive current to below-average SoC cells (Cells 1, 3, and 4) while drawing negative current from the above-average SoC cell (Cell 2).

In contrast, the pack-to-cell converter operates unidirectionally, delivering positive charging currents proportional to SoC deviation (Icharge ∝ (SoCavg - SoCcell)), whereas the cell-to-pack converter exclusively discharges cells, with current magnitude following Idisharge ∝ (SoCcell - SoCavg). This operational disparity explains the bidirectional converter's superior balancing speed, as it enables concurrent energy exchange rather than sequential charging or discharging.

B. Second Case

The State of Charge (SoC) distribution across individual cells and their respective deviations from the average value are presented in Table 7. The second case is the opposite of the first case, only Cell 4 exhibits a significantly lower SoC value compared to the other cells in the system, resulting in this cell being the sole unit with a negative deviation. The corresponding simulation results are illustrated in Fig. 13.

TABLE VII. THE SOC OF EACH SEL IN THE SECOND CASE

Cell	SoC	deviation
1	59.99 %	0.0725
2	59.98 %	0.0625
3	59.95 %	0.0325
4	59.75 %	-0.1675

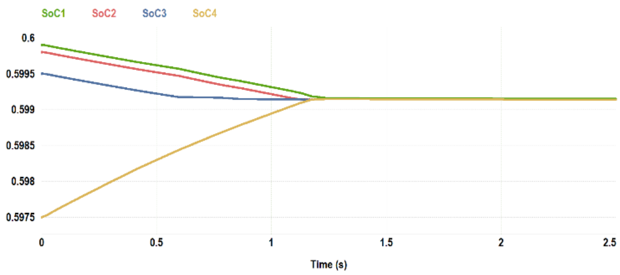

a) Battery SoC with Bidirectional Converter

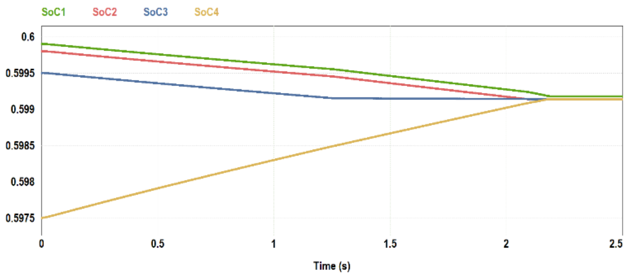

(b) Battery SoC with Pack to Cell Converter

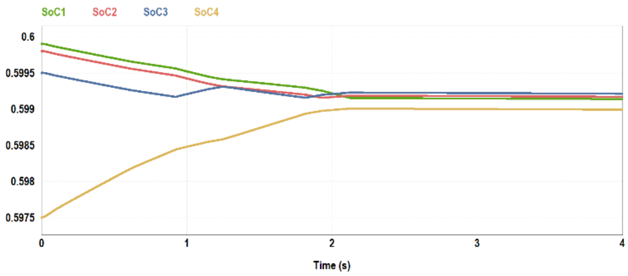

(c) Battery SoC with Cell to Pack Converter

Fig. 13. SoC of the battery in the first case

The time required to achieve balance for each controller is shown in Table 8, and the current for each cell is shown in Table 9.

TABLE VIII. THE TIME TO REACH BALANCE STATE IN THE SECOND CASE

Converter	Time (s)
Bidirectional	1.341
Pack to Cell	2.25
Cell to Pack	Not reach

TABLE IX. CURRENT OF EACH CELL IN THE SECOND CASE

Cell	Average Current (A)		
	Bidirectional	**Pack to Cell**	**Cell to Pack**
1	-2.477	0.1184	-4.061
2	-2.295	0.216	-3.837
3	-1.383	0.707	-3.257
4	4.693	3.978	-0.244

Fig. 13 and Table 8 presents the SoC-voltage characteristics for each cell in the second experimental case. The results demonstrate that the bidirectional converter maintains its superior balancing performance, achieving equilibrium in just 1.341 seconds - 40.4% faster than the pack-to-cell converter (2.25 seconds). Consistent with the first case, the cell-to-pack configuration again failed to reach balanced conditions within the experimental duration.

As evidenced in Table 9, only the bidirectional converter exhibits both positive and negative current values, confirming its unique capability for energy transfer in both directions. This bidirectional functionality directly contributes to its significantly faster balancing performance compared to unidirectional alternatives.

C. Third Case

The State of Charge (SoC) distribution across individual cells and their respective deviations from the average value are presented in Table 10. The third case is the case where two cells have values above the average and the other two are below the average.. The corresponding simulation results are illustrated in Fig. 14.

TABLE X. THE SOC OF EACH CELL IN THE THIRD CASE

Cell	SoC	deviation
1	99.20 %	-0.275
2	100.00 %	0.525
3	98.80 %	-0.675
4	99.90 %	0.425

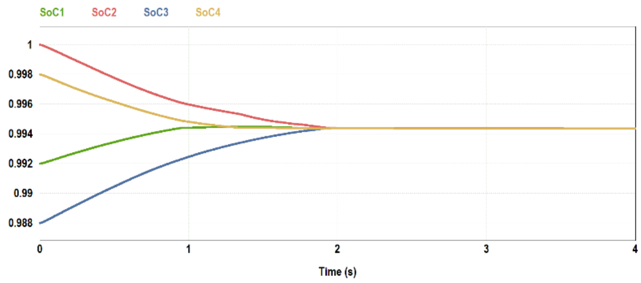

a) Battery SoC with Bidirectional Converter

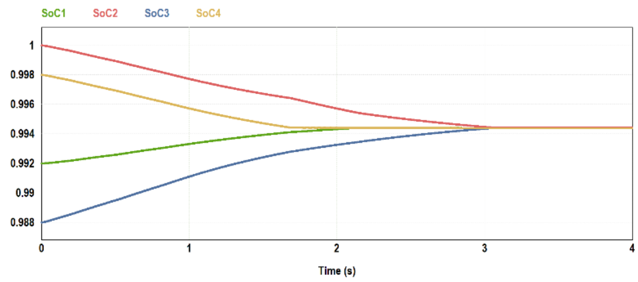

(b) Battery SoC with Pack to Cell Converter

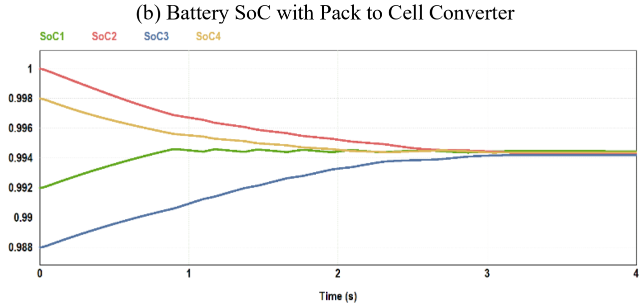

(c) Battery SoC with Cell to Pack Converter

Fig. 14. SoC of the battery in the third case

TABLE XI. THE TIME TO REACH BALANCE STATE IN THE SECOND CASE

Converter	Time (s)
Bidirectional	1.968
Pack to Cell	3.052
Cell to Pack	3.141

TABLE XII. CURRENT OF EACH CELL IN THE SECOND CASE

Cell	Average Current (A)		
	Bidirectional	Pack to Cell	Cell to Pack
1	4.783	9.994	-4.929
2	-10.113	0.648	-14.175
3	12.270	14.690	-0.670
4	-6.446	2.949	-11.872

Fig. 14 and Table 11 presents the results of the third case study, comparing the balancing performance of three converter modes. The bidirectional converter again demonstrates the fastest balancing time (1.968 seconds), outperforming both the pack-to-cell (3.052 seconds) and cell-to-pack (3.141 seconds) configurations. As in the previous case, Table 12 shows that only the bidirectional converter displays positive and negative current values, confirming its unique ability to transfer energy in both directions, resulting in faster balancing times. This consistency across multiple test cases confirms the bidirectional converter's superior effectiveness and adaptability under varying conditions.

IV. CONCLUSION

Based on three experimental cases, this study shows that bidirectional flyback converters consistently outperform unidirectional configurations (pack-to-cell and cell-to-pack) in terms of speed and adaptability LMB balancing. The bidirectional converter achieved the fastest balancing time in all cases (1.05 seconds, 1.341 seconds, and 1.968 seconds), with convergence 35–40% faster than unidirectional methods. Only the bidirectional converter successfully managed overcharged and undercharged cells simultaneously, as demonstrated by its ability to handle positive/negative current flows. The bidirectional system maintains superior performance under varying initial SoC deviations, confirming its reliability under diverse conditions. These results demonstrate that the combined use of a bidirectional flyback converter and Fuzzy Logic Control (FLC) offers an efficient solution for active balancing, particularly for high-capacity battery systems like LMB. Further research could explore real-world implementation and scalability for grid-scale applications.

ACKNOWLEDGMENT

This work is supported by the Energy Conversion Laboratory of *Institut Sepuluh Nopember* (ITS) and *Perusahaan Listrik Negara* (PLN).

REFERENCES

[1] X. Feng, M. Ouyang, X. Liu, L. Lu, Y. Xia, and X. He, "Thermal runaway mechanism of lithium ion battery for electric vehicles: A review," *Energy Storage Mater.*, vol. 10, pp. 246-267, Jan. 2018, doi: 10.1016/j.ensm.2017.05.013.

[2] [1] M. A. Hannan, M. M. Hoque, A. Mohamed, and A. Ayob, "Review of energy storage systems for electric vehicle applications: Issues and challenges," *Renew. Sustain. Energy Rev.*, vol. 69, pp. 771–789, Mar. 2017, doi: 10.1016/j.rser.2016.11.171.

[3] M. Zhao, Y. Zhou, C. Yi, and X. Ning, "High performance dual active bismuth-cadmium positive electrode for liquid metal battery," *Journal of Energy Storage,* vol. 131, no. Part A, p. 117429, 2025, doi: 10.1016/j.est.2025.117429.

[4] Y. Ding, X. Guo, dan G. Yu, "Next-Generation Liquid Metal Batteries Based on the Chemistry of Fusible Alloys," **ACS Central Science**, vol. 6, no. 8, pp. 1355–1366, 2020, doi: 10.1021/acscentsci.0c00716.

[5] T. Xu, K. Yang, Z. Song dan X. Sun, "Research on Sensorless Equalization Current Estimation of Liquid Metal Battery," *on 7th International Conference on Power and Renewable Energy (ICPRE),* 2022 Shanghai, China, 2022, pp. 1037-1042, doi: 10.1109/ICPRE55555.2022.9960659.

[6] L. Fan, E. Zhang, T. Yang, H. Li, B. Li, K. Wang, and K. Jiang, "A balancing system for liquid metal batteries using the Floyd-Warshall algorithm," *International Journal of Electrochemical Science*, vol. 20, p. 100915, Dec. 2024, doi: 10.1016/j.ijoes.2024.100915.

[7] S. R. Raman, X. D. Xue, and K. W. E. Cheng, "Review of charge equalization schemes for Li-ion battery and super-capacitor energy storage systems," *2014 Int. Conf. Adv. Electron. Comput. Commun. ICAECC 2014,* Jan. 2015, doi: 10.1109/ICAECC.2014.7002471.

[8] M. A. Gaafar, A. Mostafa, M. Orabi, M. Watanabe, and O. Abdel-Rahim, "Active balancing strategy for battery power module systems with reduced count of sensors," Journal of Power Sources, vol. 648, p. 237419, 2025, doi: 10.1016/j.jpowsour.2025.237419.

[9] R. R. Thakkar, Y. S. Rao and R. R. Sawant, "Comparative Performance Analysis on Passive and Active Balancing of Lithium-Ion Battery Cells," *2021 IEEE 18th India Council International Conference (INDICON)*, Guwahati, India, 2021, pp. 1-5, doi: 10.1109/INDICON52576.2021.9691538.

[10] Format IEEE: Y. Lee, S. Jeon, H. Lee, and S. Bae, "Comparison on Cell Balancing Methods for Energy Storage Applications," Indian Journal of Science and Technology, vol. 9, no. 17, pp. 1–8, May 2016, Art no. 92316, doi: 10.17485/ijst/2016/v9i17/92316.

[11] J.-H. Kwon, S.-C. Choi, G. Zhou, S.-M. Park, S.-J. Park, and Y. Wang, "A Cell-to-cell Voltage Balancing Strategy with Bidirectional Flyback Converter," *2024 IEEE 10th International Power Electronics and Motion Control Conference (IPEMC2024-ECCE Asia),* Chengdu, China, 2024, pp. 4088–4093, doi: 10.1109/IPEMC-ECCEAsia60879.2024.10567312.

[12] S. M. P and A. M. Parimi, "Design of an isolated bidirectional active cell balancing circuit for lithium ion batteries," *2022 IEEE 7th International Conference for Convergence in Technology (I2CT)*, Mumbai, India, 2022, pp. 1-6, doi: 10.1109/I2CT54291.2022.9825103.

[13] L. Chen, Z. Lai, A. M. Lopes, X. Dong, and Y. Chen, "Modular balancing strategy for lithium battery pack based on adaptive fuzzy logic control and energy path optimization," *Journal of Energy Storage*, vol. 91, p. 112073, 2024, doi: 10.1016/j.est.2024.112073.

[14] X. Wang, L. Wang, Z. Li, and G. Chen, "State of charge estimation for liquid metal battery using Kalman filter," *in _2017 IEEE Conference on Energy Conversion (CENCON)_*, Kuala Lumpur, Malaysia, 2017, pp. 67–72, doi: 10.1109/CENCON.2017.8262460.

[15] Y. Zhang, Z. Guo, Y. He, and M. Zhou, "Thermal simulation for a 200 Ah Li||Bi liquid metal battery," *in _2022 4th International Conference on Smart Power & Internet Energy Systems (SPIES)*, Beijing, China, 2022, pp. 1783-1787, doi: 10.1109/SPIES55999.2022.10082159

[16] T. Xu, K. Yang, Z. Song, and X. Sun, "Research on sensorless equalization current estimation of liquid metal battery," in _2022 7th *International Conference on Power and Renewable Energy (ICPRE)*_, Shanghai, China, 2022, pp. 1037–1042, doi: 10.1109/ICPRE55555

[17] G. Chu, H. Wen, L. Jiang, Y. Hu, and X. Li, "Bidirectional flyback based isolated-port submodule differential power processing optimizer for photovoltaic applications," **Solar Energy**, vol. 158, pp. 929-940, Dec. 2017, doi: 10.1016/j.solener.2017.10.053.

[18] M.N. Cirstea, A. Dinu, J.G. Khor, dan M. McCormick, "Neural and Fuzzy Logic Control of Drives and Power Systems", Newnes, 2002